

# Reversible Phototuning of Ferromagnetism at Au–S Interfaces at Room Temperature\*\*

Masayuki Suda, Naoto Kameyama, Motohiro Suzuki, Naomi Kawamura, and Yasuaki Einaga\*

The design of molecular compounds that exhibit photo-induced magnetization and magnetic transitions is one of the main challenges in the field of materials science because of their possible application to future optical memory and switching devices. Photoinduced changes in magnetic order have been studied extensively in a variety of systems, including cyanometalate-based compounds,<sup>[1–3]</sup> LIESST (light-induced excited spin-state trapping) compounds,<sup>[4–6]</sup> diluted magnetic semiconductors,<sup>[7,8]</sup> and manganite films.<sup>[9]</sup> Although interesting photomagnetic phenomena have been reported in the above systems, most of the observations of such phenomena have been limited to operation at very low temperature. Other candidate systems that show photomagnetic effects occur in hybrid materials of organic photochromes and inorganic magnetic compounds whose magnetic properties are relatively superior to those of conventional compounds.<sup>[10–14]</sup> Based on such a strategy, a previous report has demonstrated room-temperature reversible photocontrol of ferromagnetic order in photochrome-modified FePt nanoparticles.<sup>[15]</sup> However, the occurrence of these photomagnetic effects was limited to just the surface layers of the FePt nanoparticles. Hence, the design and synthesis of a new class of optically switchable magnetic compounds that exhibit both large magnetization changes and ferromagnetic order even at room temperature is still a challenging issue.

Herein we propose a novel strategy that focuses on the two-dimensional ferromagnetism which appears “out of nowhere” at the interfaces between organic–inorganic hybrids such as self-assembled monolayer (SAM) films on gold. In a number of recent papers, the occurrence of ferromagnetism at Au–S interfaces has been observed.<sup>[16–19]</sup> The ferromagnetism has been associated with Au 5d localized holes that are the result of charge transfer from the Au surface

atoms to the S atoms of the organic ligands when forming the Au–S bonds. Since charge transfer from Au to S atoms acts as a “trigger” for the generation of ferromagnetism, the magnitudes of the magnetic moments will vary with the metal work functions. It is well known that the metal work function is correlated with the surface dipole of organic layers, which arises from the cooperative effect of intrinsic molecular dipole moments.<sup>[20]</sup> Since the *trans* state and *cis* state of azobenzene-derivatized thiols have opposite dipoles, they can be used to decrease and increase the work function of gold, respectively. As a consequence, the use of SAM-containing photochromes grafted onto gold surfaces has been shown to have great potential for the photocontrol of magnetic properties. Furthermore, reducing the volume of such materials down to the nanometer scale will expose the local ferromagnetic areas at the Au–S interfaces as explicit entities, which will not only leads to enhancement of the magnetism, but also opens the possibility that the magnetization could be controllable by photochromes with high efficiency. We now report reversible photoinduced magnetization changes that were observed in gold nanoparticles passivated with azobenzene-derivatized ligands.

Figure 1 shows TEM images and size distribution histograms for the AZ-passivated gold nanoparticles (AZ-Au

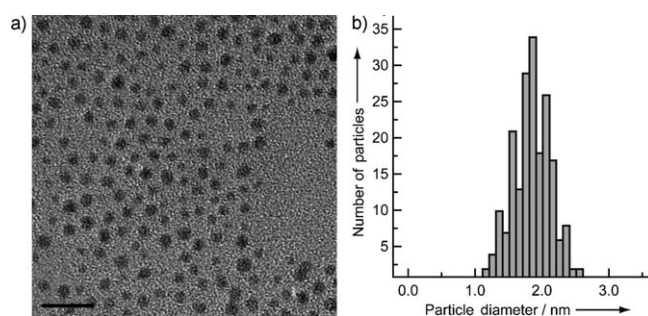
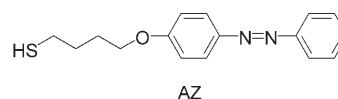


**Figure 1.** a) TEM micrograph of AZ-Au NPs deposited from a toluene dispersion onto a collodion-coated copper grid; scale bar: 10 nm. b) Size distribution of the AZ-Au NPs; the average was determined to be  $1.74 \pm 0.29$  nm.



NPs) prepared by the modified Brust method.<sup>[21]</sup> The AZ-Au NPs exhibit a narrow size distribution with an average size of  $1.74 \pm 0.29$  nm. The powder X-ray diffraction pattern of the AZ-Au NPs (shown in the Supporting Information) is consistent with a face-centered cubic crystal structure for Au

[\*] M. Suda, N. Kameyama, Prof. Y. Einaga  
Department of Chemistry  
Faculty of Science and Technology  
Keio University  
3-14-1 Hiyoshi, Yokohama 223-8522 (Japan)  
Fax: (+81) 45-566-1697  
E-mail: einaga@chem.keio.ac.jp

Dr. M. Suzuki, Dr. N. Kawamura  
Japan Synchrotron Radiation Research Institute (JASRI/SPRING-8)  
1-1-1 Kouto, Sayo, 679-5198 (Japan)

[\*\*] This work was supported by the New Energy and Industrial Technology Development Organization (NEDO) and a Grant-in-Aid for Scientific Research from the Ministry of Education, Culture, Sports, Science and Technology (MEXT) of the Japanese government.

Supporting information for this article is available on the WWW under <http://www.angewandte.org> or from the author.

with lattice constant  $a = 2.33 \text{ \AA}$ . The average particle size, determined from the instrument-corrected width  $\beta$  using the Scherrer relation ( $D = K\lambda/\beta\cos\theta$ ), is 1.8 nm, which is in good agreement with the results from the TEM studies.

Figure 2a shows the X-ray absorption near-edge structure (XANES) spectra of the Au  $L_3$  edge for both the AZ-Au NPs

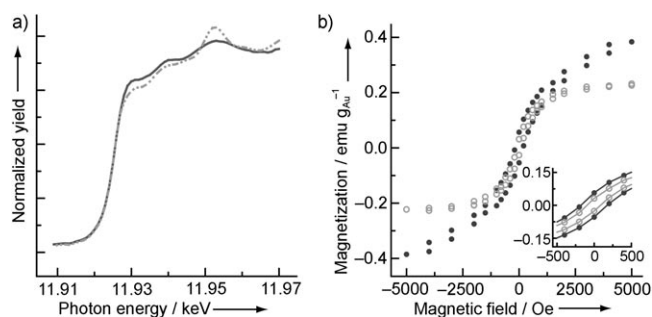


**Figure 2.** a) Au  $L_3$  edge XANES spectra for the AZ-Au NPs (solid line) and gold foil (dashed line). b) Plot of magnetization  $M$  versus applied magnetic field  $H$  at 300 K (open circles) and at 5 K (filled circles). The inset shows a magnified view with low field and low magnetization scales.

and bulk Au (foil).<sup>[22]</sup> Typical XANES spectra of an fcc gold structure exhibit patterns with three peaks within the first 40 eV above the edge. The first resonance at the threshold (known as “white line”) associated with  $2p_{3/2}$  to  $5d_{5/2,3/2}$  dipole transitions probes the density of the unoccupied d states (d-hole counts) at the Fermi level.<sup>[23]</sup> Although the 5d orbitals of bulk Au are nominally full, a small concentration of itinerant holes at the d band can be detected in the XANES spectra of bulk Au owing to spd-level hybridization. In the case of the AZ-Au NPs, a noticeable increase in the threshold resonance was detected when compared to the bulk Au, indicating a loss in 5d electron density owing to d-charge transfer from the gold to the sulfur atoms.

The magnetization curves ( $M$ – $H$  plots) measured at 300 and 5 K for AZ-Au NPs with an inset showing a magnified view are shown in Figure 2b. Typical hysteresis loops with coercivity ( $H_c$ ) and remanent magnetization ( $M_r$ ) were observed even at 300 K. Similar observations were reported for dodecanthiol-capped 1.4-nm Au nanoparticles.<sup>[17]</sup> The values of  $H_c$  and  $M_r$  were 100 G and  $0.031 \text{ emu g}_{\text{Au}}^{-1}$  at 300 K and 200 G and  $0.057 \text{ emu g}_{\text{Au}}^{-1}$  at 5 K.

The photoisomerization of AZ-Au NPs in the solid state at room temperature was monitored by UV/Vis absorption spectroscopy (Figure 3a). The spectrum of the initial state gave an intense absorption peak at 360 nm, which is ascribed to the  $\pi$ – $\pi^*$  transition in the *trans* isomer of the azo ligands. After UV illumination of the *trans* isomer for 1 min, the absorption at 360 nm decreased. After subsequent illumination with visible light, the absorption at 360 nm increased again. After the second cycle, the *cis*–*trans* photoisomerization was repeated without any attenuation of the area between the curves. These reversible spectral changes indicate high-efficiency reversible photoisomerization, even in the solid state. Normally, photoisomerization of azobenzene-

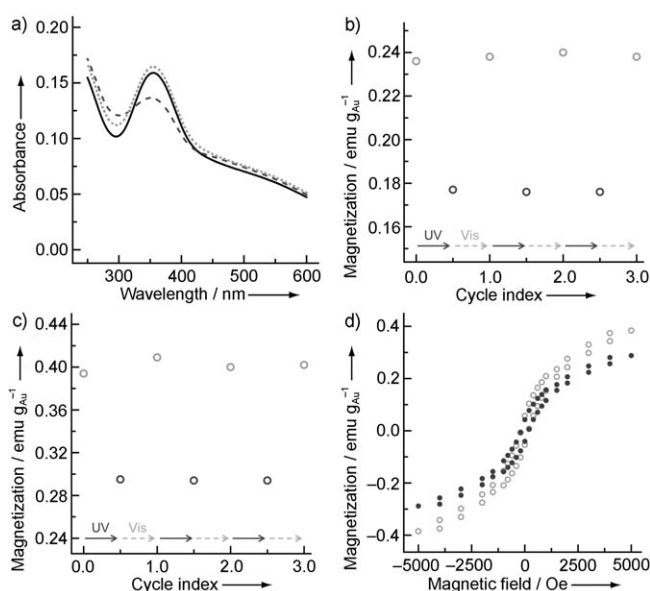


**Figure 3.** a) Changes in the optical absorption spectra for AZ-Au NPs as a result of photoisomerization. The initial *trans* state (solid line) was first illuminated with UV light for 1 min (dashed line). It was then illuminated with visible light for 1 min (dotted line). b) Changes in magnetization by photoillumination at 300 K; the AZ-Au NPs were alternately illuminated with UV and visible light for 1 min each at 300 K under an external magnetic field of 5 T. c) Changes in magnetization by photoillumination at 5 K; the AZ-Au NPs were alternately illuminated with UV and visible light for 1 min each at 5 K with an external magnetic field of 5 T. d) Changes in magnetization curves at 5 K; plot of magnetization  $M$  versus applied magnetic field  $H$  for the *trans* state (open circles) and for the *cis* state (filled circles).

containing compounds does not occur in the solid state because of the large volume changes that are involved.<sup>[24]</sup> In fact, photoisomerization also does not occur in the absence of spacers when azobenzene-containing ligands are self-assembled on two-dimensional gold films.<sup>[25]</sup> However, in the system presented here, with an average particle diameter of 1.74 nm, reversible photoisomerization was observed in the solid state with high efficiency.

From the above observations, it is proposed that the decrease in particle size provides free volume between each of the AZ ligands because the adjacent angles between two neighboring AZ ligands would be increased with decreasing particle size. The average distance between two neighboring nitrogen double bonds on the AZ ligands could be estimated as  $5.0 \text{ \AA}$  for an azobenzene-containing SAM, while it was estimated as  $13.0 \text{ \AA}$  for 1.74-nm particles (a schematic illustration is available in the Supporting Information).

Another important aspect concerning the optical absorption spectra of AZ-Au NPs (Figure 3a) is the absence of any surface plasmon resonance, which indicates the existence of strong interactions between the surface gold atoms and the adsorbate. These strong Au–S interactions make the 5d electrons of the core gold nanoparticles behave as partially localized holes that have lost itinerancy.<sup>[17,22]</sup> The above observations are consistent with the observed d-charge transfer derived from the results of the XANES measurements and the observed ferromagnetism from the SQUID measure-

ments. After all, reducing the particle size to 1.74 nm enhances not only the magnetic properties, but also the photoisomerization efficiency of AZ-Au NPs.

Subsequently, we investigated the influence of photoillumination on the magnetic properties of AZ-Au NPs at 300 K (Figure 3b). During the UV illumination, the initial magnetization value under an applied field of 5 T decreased from 0.24 to 0.18 emu<sub>Au</sub><sup>-1</sup>. Even after the illumination was stopped, the decreased magnetization value was maintained for several hours at room temperature. The very slow recovery of the magnetization could be due to the *cis*-to-*trans* thermal back-isomerization of the AZ moiety. We then illuminated the AZ-Au NPs with visible light, and the magnetization value increased from 0.18 to 0.24 emu<sub>Au</sub><sup>-1</sup>. After this process, the UV-light-induced decrease and the visible-light-induced increase in magnetization were repeated without any attenuation. The photoinduced changes in the magnetization values were estimated to be about 27%. We also observed such photoinduced magnetic transitions in the AZ-Au NPs even at 5 K with almost the same efficiency of about 25% (Figure 3c). Because the thermal back-isomerization of the AZ ligands did not occur at low temperature, we also observed significant changes in the magnetization curves at 5 K (Figure 3d).

As mentioned above, in Au NPs, the apparent ferromagnetism is associated with 5d localized holes in the 5d shell that are generated through Au–S bonding. The magnetic ordering is not due to the large exchange interaction, but rather is due to extremely high local magnetic anisotropy (estimated to be as high as  $1 \times 10^8$  erg cm<sup>-3</sup>), which blocks the moments from switching, resulting in very high  $T_B$  (blocking temperature) values in Au NPs.<sup>[17]</sup> From the saturated magnetization value of the AZ-Au NPs under an applied field of 5 T at 5 K, an estimation of the lower limit value of the magnetic moment of the gold atoms is straightforward. The values of the magnetic moment per Au atom bound to sulfur in the *trans* state and the *cis* state are estimated to be 0.033  $\mu_B$  and 0.024  $\mu_B$ , respectively. In a recent report concerning an XMCD (X-ray magnetic circular dichroism) study of thiolated gold clusters, a considerable orbital magnetic moment of the Au 5d electrons was indicated, and the ratio of the orbital magnetic moment to the spin magnetic moment was estimated to be 12%.<sup>[18]</sup> Therefore, the lower limit value of the d-hole counts per Au atom bound to sulfur in the *trans* state and the *cis* state are estimated as to be about 0.0039 and 0.0027 e atom<sup>-1</sup>, respectively. This result clearly suggests that the d-charge loss of about 0.0012 e atom<sup>-1</sup> was decreased in the case of the *cis* state, that is, the charge transfer from Au to S could be reversed with *trans*-to-*cis* photoisomerization.

These phenomena are also consistent with the reported cooperative effect of organic molecules in the electron transfer between a metal substrate and organic layers. In such organic–inorganic interfaces, charge transfer acts to reduce the dipole–dipole interaction between molecules but

may either decrease or increase the molecule-to-surface dipole moment.<sup>[26]</sup> The change in the work function is related to the dipole moment density perpendicular to the surface through the relationship given in Equation (1).<sup>[26]</sup>

$$\Delta\Phi = \frac{\mu N \cos\theta}{\epsilon\epsilon_0} \quad (1)$$

In other words, the magnitude of the electron transfer to the organic layer becomes smaller for adsorbates with electronegative end groups, while it becomes larger for adsorbates with electropositive end groups. In fact, experimental evidence for such changes in the magnitude of the electron transfer from gold to the adsorbates has been reported previously.<sup>[27]</sup>

In the system presented here, the values of  $\mu\cos\theta$  for the AZ ligands were calculated as  $-0.20$  D (D = Debye) for the *trans* state and  $2.74$  D for the *cis* state, meaning that the sign of the work function change would be negative for the *trans* state and positive for the *cis* state.<sup>[28]</sup> Hence, the magnitude of electron transfer in the initial *trans* state becomes smaller in the *cis* state under UV illumination, and it recovers to its initial value under illumination with visible light. Schematic illustrations of the changes in the work function resulting from the photoisomerization of AZ are shown in Figure 4. As a consequence, the magnetization values could be controlled by employing alternating photoillumination with UV and visible light, as caused by changes in the d-charge loss owing to the photoisomerization of AZ ligands.

In conclusion, we have designed azobenzene-passivated ferromagnetic gold nanoparticles whose magnetic moments are localized at the organic–inorganic interfaces. The magnetic properties of these compounds could be controlled by alternating photoillumination with UV and visible light in the

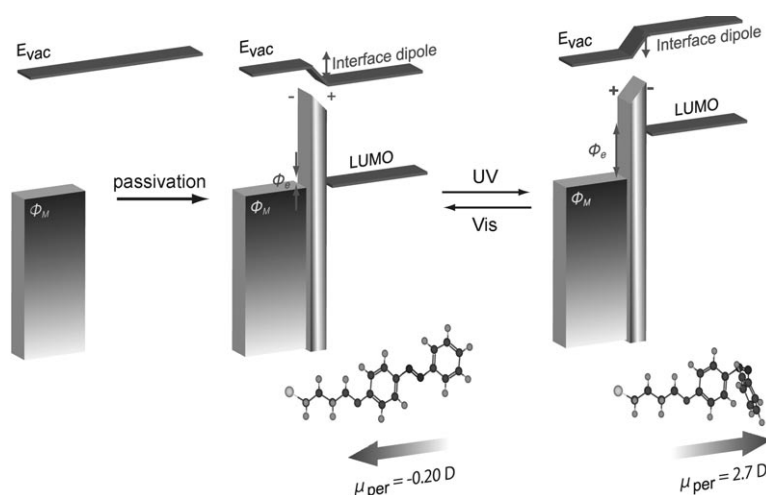


**Figure 4.** Schematic illustrations of changes in the work function resulting from photoisomerization of AZ; left: schematic energy-level diagrams for an untreated interface (without surface passivation); middle: passivation of *trans*-AZ imposes an interface dipole that decreases the local vacuum energy level ( $E_{vac}$ ); right: photoisomerization to *cis*-AZ imposes an interface dipole that increases the local vacuum energy level ( $E_{vac}$ ).  $\mu_{per}$  is the vertical component of the surface dipole,  $\Phi_M$  is the metal work function, and  $\Phi_e$  is the electron injection barrier.

solid state even at room temperature. The changes in the magnetization values were significant, and were estimated to be around 27%. Furthermore, in recent years there has been much interest in energy-level alignment in various types of organic–inorganic interfaces.<sup>[20,29,30]</sup> Thus, the novel strategy presented here not only becomes the basis for developing future magneto-optical memory, but also has great potential for developing new classes of materials.

Received: September 1, 2007

Published online: November 8, 2007

**Keywords:** azo compounds · gold · magnetic properties · nanostructures · photochromism

- [1] O. Sato, T. Iyoda, A. Fujishima, K. Hashimoto, *Science* **1996**, 272, 704.
- [2] S. Ohkoshi, S. Yoroze, O. Sato, T. Iyoda, A. Fujishima, K. Hashimoto, *Appl. Phys. Lett.* **1997**, 70, 1040.
- [3] T. Yamamoto, Y. Umemura, O. Sato, Y. Einaga, *J. Am. Chem. Soc.* **2005**, 127, 16065.
- [4] S. Decurtins, P. Güttlich, C. P. Kohler, H. Spiering, A. Hauser, *Chem. Phys. Lett.* **1984**, 105, 1.
- [5] F. Renz, H. Oshio, V. Ksenofontov, M. Waldeck, H. Spiering, P. Güttlich, *Angew. Chem.* **2000**, 112, 3832; *Angew. Chem. Int. Ed.* **2000**, 39, 3699.
- [6] S. Hayami, Z. Z. Gu, M. Shiro, Y. Einaga, A. Fujishima, K. Hashimoto, *J. Am. Chem. Soc.* **2000**, 122, 7126.
- [7] S. Koshihara, A. Oiwa, M. Hirasawa, S. Katsumoto, Y. Iye, C. Urano, H. Takagi, H. Muneoka, *Phys. Rev. Lett.* **1997**, 78, 4617.
- [8] S. Haneda, H. Muneoka, Y. Takatani, S. Koshihara, *J. Appl. Phys.* **2000**, 87, 6445.
- [9] K. Matsuda, A. Machida, Y. Moritomo, A. Nakamura, *Phys. Rev. B* **1998**, 58, R4203.
- [10] Y. Einaga, O. Sato, T. Iyoda, A. Fujishima, K. Hashimoto, *J. Am. Chem. Soc.* **1999**, 121, 3745.
- [11] R. Mikami, M. Taguchi, K. Yamada, K. Suzuki, O. Sato, Y. Einaga, *Angew. Chem.* **2004**, 116, 6261; *Angew. Chem. Int. Ed.* **2004**, 43, 6135.
- [12] M. Suda, Y. Miyazaki, Y. Hagiwara, O. Sato, S. Shiratori, Y. Einaga, *Chem. Lett.* **2005**, 34, 1028.
- [13] S. Benard, E. Riviere, P. Yu, *Chem. Mater.* **2001**, 13, 159.
- [14] M. Okubo, M. Enomoto, N. Kojima, *Synth. Met.* **2005**, 152, 461.
- [15] M. Suda, M. Nakagawa, T. Iyoda, Y. Einaga, *J. Am. Chem. Soc.* **2007**, 129, 5538.
- [16] I. Carmeli, G. Leituss, R. Naaman, S. Reich, Z. Vager, *J. Chem. Phys.* **2003**, 118, 10372.
- [17] P. Crespo, R. Litrán, T. C. Rojas, M. Multigner, J. M. de la Fuente, J. C. Sánchez-López, M. A. García, A. Hernando, S. Penadés, A. Fernández, *Phys. Rev. Lett.* **2004**, 93, 087204.
- [18] Y. Negishi, H. Tsunoyama, M. Suzuki, N. Kawamura, M. M. Matsushita, K. Maruyama, T. Sugawara, T. Yokoyama, T. Tsukuda, *J. Am. Chem. Soc.* **2006**, 128, 12034.
- [19] P. Dutta, S. Pal, M. S. Seehra, M. Anand, C. B. Roberts, *Appl. Phys. Lett.* **2007**, 90, 213102.
- [20] H. Ishii, K. Sugiyama, E. Ito, K. Seki, *Adv. Mater.* **1999**, 11, 605.
- [21] M. Brust, M. Walker, D. Bethell, D. J. Schiffrin, R. Whyman, *J. Chem. Soc. Chem. Commun.* **1994**, 801.
- [22] The XANES spectra were recorded using a spectrometer installed in BL39XU at the SPring-8 Synchrotron Radiation Facilities in Sayo, Japan.
- [23] P. Zhang, T. K. Sham, *Phys. Rev. Lett.* **2003**, 90, 244502.
- [24] H. Nakahara, K. Fukuda, M. Shimomura, T. Kunitake, *Nippon Kagaku Kaishi* **1988**, 7, 1001.
- [25] S. D. Evans, S. R. Johnson, H. Ringsdorf, L. M. Williams, H. Wolf, *Langmuir* **1998**, 14, 6436.
- [26]  $N$  is the surface density of dipoles,  $\mu$  is the effective dipole moment of the molecule,  $\epsilon_0$  is the permittivity of a vacuum,  $\epsilon$  is the dielectric constant of the layer, and  $\theta$  is the tilt angle of the molecule with respect to the surface normal.
- [27] S. G. Ray, H. Cohen, R. Naaman, H. Liu, D. H. Waldeck, *J. Phys. Chem. B* **2005**, 109, 14064.
- [28] The  $\mu \cos \theta$  values of AZ ligands for the *trans* state and *cis* state were calculated with ZINDO CI at MM/PM3 geometry using a CAChe Workspace (Fujitsu). The tilt angles were taken to be 30° for both *trans* state and *cis* state.
- [29] R. Cohen, L. Kronik, A. Shanzer, D. Cahen, A. Liu, Y. Rosenwaks, J. K. Lorenz, A. B. Ellis, *J. Am. Chem. Soc.* **1999**, 121, 10545.
- [30] I. Carmeli, F. Bloom, E. G. Gwinn, T. C. Kreutz, C. Scoby, A. C. Gossard, *Appl. Phys. Lett.* **2006**, 89, 112508.